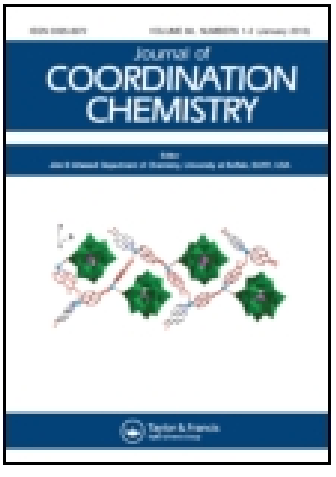

Journal of Coordination Chemistry
Publication details, including instructions for authors and subscription information:
http://www.tandfonline.com/loi/gcoo20

Synthesis, crystal structure, and properties of cobalt, zinc, and manganese coordination polymers based on fluconazole

Gang-Hong Pan[a], Jing-Niu Tang[a], Xian-Hong Yin[a], Peng-Fei Li[a] & Zhong-Jing Huang[a]

[a] College of Chemistry and Chemical Engineering, Guangxi University for Nationalities, Nanning, PR China

Accepted author version posted online: 13 Jun 2014.Published online: 10 Jul 2014.

To cite this article: Gang-Hong Pan, Jing-Niu Tang, Xian-Hong Yin, Peng-Fei Li & Zhong-Jing Huang (2014) Synthesis, crystal structure, and properties of cobalt, zinc, and manganese coordination polymers based on fluconazole, Journal of Coordination Chemistry, 67:11, 1962-1979, DOI: 10.1080/00958972.2014.934229

To link to this article: http://dx.doi.org/10.1080/00958972.2014.934229

Journal of Coordination Chemistry, 2014
Vol. 67, No. 11, 1962–1979, http://dx.doi.org/10.1080/00958972.2014.934229

Synthesis, crystal structure, and properties of cobalt, zinc, and manganese coordination polymers based on fluconazole

GANG-HONG PAN, JING-NIU TANG, XIAN-HONG YIN, PENG-FEI LI and ZHONG-JING HUANG*

College of Chemistry and Chemical Engineering, Guangxi University for Nationalities, Nanning, PR China

(*Received 29 August 2013; accepted 1 May 2014*)

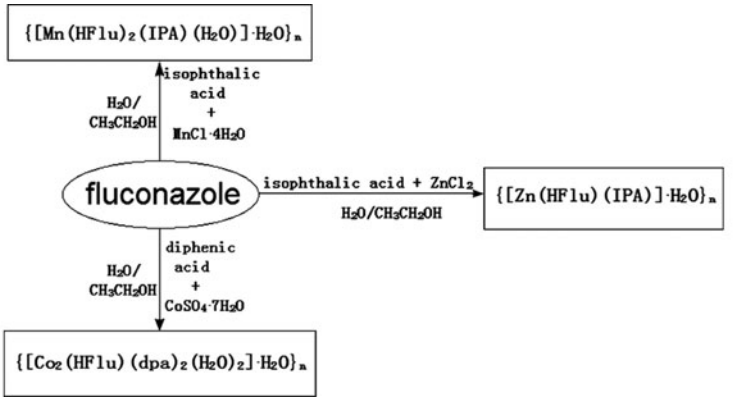

Three complexes based on fluconazole, namely, $\{[Co_2(HFlu)(dpa)_2(H_2O)_2]\cdot H_2O\}_n$ (**1**), $\{[Zn(HFlu)(IPA)]\cdot H_2O\}_n$ (**2**), and $\{[Mn(HFlu)_2(IPA)(H_2O)]\cdot H_2O\}_n$ (**3**) (HFlu = fluconazole, 2-(2,4-difluoro-phenyl)-1,3-bis(1,2,4-triazol-1-yl)-propan-2-ol; H_2dpa = diphenic acid; H_2IPA = isophthalic acid) have been synthesized. Single-crystal X-ray analysis revealed that **1** is a 2-D-network framework containing a trinuclear Co(II) unit, **2** is a 3-D framework, and **3** is 1-D double chain structure with a Mn_2 metallocyclic core. The complexes have also been characterized by elemental analyses, IR, UV/vis and fluorescence spectroscopy, and thermal gravimetry. The phase purity of these polymers has been confirmed via powder X-ray diffraction.

Keywords: Coordination polymer; Fluconazole; UV/vis spectra; Fluorescence; Thermal gravimetry

1. Introduction

The design and synthesis of metal–organic framework complexes are of great current interest due to their intriguing architectures, topologies, and potential applications in catalysis, luminescence, ion exchange, and gas storage [1–8]. Therefore, a search for rational synthetic strategies for these complexes is an important task. One of these strategies involves the use of ligands

*Corresponding author. Email: pgh1919@163.com

with numerous coordination sites. Fluconazole [2-(2,4-difluorophenyl)-1,3-di(1H-1,2,4-triazol-1-yl)propan-2-ol, HFlu] is known as an antifungal drug which was first synthesized and reported in the scientific literature by Richardson *et al.* as the outcome of their research initiated in 1970 [9, 10]. HFlu as a ligand shows interesting coordinating characteristics, affording extended networks in a head-to-tail mode with good flexibility through rotation and twisting of the C–C and C–N bonds [11–14]. HFlu can chelate to metal ions via endodentate nitrogen atoms and an alkoxy oxygen atom to form binuclear complexes [15]. Furthermore, the HFlu ligand has several available donors/acceptors (2,4-difluorophenyl and hydroxyl groups) to form weak interactions to stabilize the supramolecular frameworks [11–21].

Along these lines, we report three coordination polymers, $\{[Co_2(HFlu)(dpa)_2(H_2O)_2]\cdot H_2O\}_n$ (**1**), $\{[Zn(HFlu)(IPA)]\cdot H_2O\}_n$ (**2**), and $\{[Mn(HFlu)_2(IPA)(H_2O)]\cdot H_2O\}_n$ (**3**). (H_2dpa = diphenic acid; H_2IPA = isophthalic acid). Single-crystal X-ray analysis revealed that **1** is a 2-D structure with trinuclear Co(II) units, showing an –ABAB– sequence. Water molecules are present between the layers and further stabilize the structural framework through extensive hydrogen bonding. Complex **2** is a 3-D framework. Complex **3** is 1-D double chain structure with a Mn_2 metallocyclic core. The IR, UV/vis and fluorescence spectroscopy, and thermal gravimetry of these complexes have also been studied.

2. Experimental

All chemicals were commercial materials of analytical grade and used as received. The FT-IR spectra were obtained on a Nicolet 520 FT-IR spectrophotometer in the 4000–400 cm^{-1} regions, using KBr pellets. C, H, N elemental analyses were carried out on a Perkin-Elmer 2400 II elemental analyzer. Powder X-ray diffraction (PXRD) patterns were obtained using a pinhole camera (Anton Paar) operating with point focused, Ni-filtered CuK_α radiation in the 2θ range from 5° to 50° with a scan rate of 0.08° s^{-1}. The optical properties were analyzed by UV/vis diffuse reflectance spectroscopy using a UV/vis spectrophotometer (Cary-500, Varian Co.), in which $BaSO_4$ was used as the internal standard. Fluorescence spectra were recorded with an F-2500 FL Spectrophotometer analyzer. Thermogravimetry analyses were performed on Perkin-Elmer TG/DTA 6300 thermal analyzer under a nitrogen atmosphere at a heating rate of 10 °C min^{-1} in the temperature range of 30–1000 °C.

2.1. *Preparation of $\{[Co_2(HFlu)(dpa)_2(H_2O)_2]\cdot H_2O\}_n$ (1)*

A mixture of fluconazole (153 mg, 0.5 mM), diphenic acid (120 mg, 0.5 mM), $CoSO_4\cdot 7H_2O$ (281 mg, 1.0 mM), 15 mL H_2O, and 3 mL ethanol was adjusted to pH 5 by dropwise addition of an aqueous solution of sodium hydroxide, then sealed in a 30 mL Teflon-lined stainless steel container. The mixture was kept under autogenous pressure at 150 °C for 3 days before cooling to room temperature at a rate of 5 °C h^{-1}. Light red crystals (0.157 g, 65.6% yield) were isolated, washed with alcohol three times, and dried in a vacuum desiccator over silica gel. Elem. Anal. Calcd (%) for $C_{41}H_{34}Co_2F_2N_6O_{12}$: C 51.37, H 3.58, N 8.77. Found: C 51.21, H 3.46, N 8.93. IR (KBr, cm^{-1}): 3420w, 3139w, 1617m, 1575s, 1541s, 1526s, 1507m, 1419w, 1396s, 1386s, 1279m, 1132m, 1117w, 988w, 966w, 751w, 676m, 655w.

2.2. *Preparation of {[Zn(HFlu)(IPA)]·H_2O}$_n$ (2)*

The same synthetic procedure as that for **1** was used except that diphenic acid and $CoSO_4·7H_2O$ were replaced by isophthalic acid (83 mg, 0.5 mM) and $ZnCl_2$ (136 mg, 1.0 mM). Yield: 0.1941 g, 70.1%. Elem. Anal. Calcd (%) for $C_{21}H_{18}F_2N_6O_6Zn$: C 45.55, H 3.28, N 15.18. Found: C 45.46, H 3.17, N 15.31. IR (KBr, cm^{-1}): 3430w, 3159w, 3122w, 1611s, 1566s, 1498w, 1477w, 1356s, 1274m, 1131m, 1040w, 988w, 964w, 889w, 841w, 740m, 674m, 658m, 622w.

2.3. *Preparation of {[Mn(HFlu)$_2$(IPA)(H_2O)]·H_2O}$_n$ (3)*

The same synthetic procedure as that for **1** was used except that diphenic acid and $CoSO_4·7H_2O$ were replaced by isophthalic acid (83 mg, 0.5 mM) and $MnCl_2·4H_2O$ (198 mg, 1.0 mM). Yield: 0.1458 g, 67.2%. Elem. Anal. Calcd (%) for $C_{34}H_{32}F_4MnN_{12}O_8$: C 47.06, H 3.72, N 19.37. Found: C 46.95, H 3.53, N 19.24. IR (KBr, cm^{-1}): 3136w, 3074s, 1624s, 1558m, 1521s, 1507m, 1429m, 1376s, 1275s, 1144w, 1127m, 967m, 748m, 676s, 658m.

2.4. *X-ray data collection and structure refinement*

X-ray diffraction data were collected on a Bruker SMART CCD diffractometer equipped with graphite-monochromatized MoK_α radiation ($\lambda = 0.71073$ Å) at 296(2) K. A high quality crystal of each complex was selected and mounted on a glass fiber. Data-sets were collected with the ω scan technique. Empirical absorption corrections were applied using the SADABS program [22]. The structures were solved by direct methods and all non-hydrogen atoms were refined with anisotropic thermal parameters by a full-matrix least-squares refinement based on F^2 using the SHELXTL package [23]. Hydrogen atoms of water molecules were located from the different Fourier maps, and the thermal factors were set to 1.2 times that of their carrier atoms. All other hydrogen atoms were placed by geometrical considerations and were added to the structure factor calculation. Further refinement details of the structural analysis for the complexes are given in table 1.

Table 1. Crystal and structure refinement data for **1–3**.

Identification code	**1**	**2**	**3**
Empirical formula	$C_{41}H_{34}Co_2F_2N_6O_{12}$	$C_{21}H_{18}F_2N_6O_6Zn$	$C_{34}H_{32}F_4MnN_{12}O_8$
Formula weight	958.60	553.78	867.66
Crystal system	Triclinic	Orthorhombic	Triclinic
Space group	$P\bar{1}$	*Pna2(1)*	$P\bar{1}$
a (Å)	10.2431(9)	22.3014(4)	10.81800(10)
b (Å)	14.06540(10)	16.89100(10)	13.7438(5)
c (Å)	14.0892(2)	6.07420(10)	14.0469(2)
α (°)	93.793(5)	90	76.765(3)
β (°)	90.314(8)	90	69.394(6)
γ (°)	93.311(8)	90	77.952(4)
Volume (Å^3), *z*	2021.96(18), 2	2288.11(6), 4	1884.04(8), 2
Calcd density (g cm^{-3})	1.575	1.608	1.529
Absorption coefficient (mm^{-1})	0.902	1.141	0.439
F (0 0 0)	980	1128	890
Data/restraints/parameters	7012/24/572	3967/7/326	6545/0/534
Goodness-of-fit on F^2	1.034	1.061	1.044
Final R^a indices [$I > 2\sigma(I)$] R_1, wR_2	0.0768, 0.1895	0.0673, 0.1333	0.0523, 0.1429
R indices (all data) R_1, wR_2	0.1322, 0.2271	0.0940, 0.1427	0.0747, 0.1678

[a] $R_1 = \sum||F_o| - |F_c||/\sum|F_o|$, $wR_2 = \left[\sum\left[w\left(F_o^2 - F_c^2\right)^2\right] \Big/ \sum\left[w\left(F_o^2\right)^2\right]\right]^{1/2}$.

3. Results and discussion

3.1. *Crystal structure descriptions*

Selected bond distances and angles for **1–3** are listed in table 2 and hydrogen bonding parameters in table 3. A single-crystal X-ray diffraction analysis revealed that **1** crystallizes in the triclinic $P\bar{1}$ space group. In the asymmetric unit, there are three Co(II) atoms, one HFlu ligand, two dpa^{2-} ligands, one coordinated water molecule, and one free water molecule. The three Co^{2+} ions are crystallographically independent. Both Co1 and Co3 are located on inversion centers with 0.5 occupancy. As shown in figure 1, Co1 is six-coordinated by six O atoms (O6, O6A, O9, O9A, O10, O10A) from six carboxylate groups of four different dpa^{2-} ligands in a slightly distorted octahedral coordination geometry. The

Table 2. Selected bond lengths (Å) and angles (°) for **1–3**.

1			
Co(1)–O(6)	2.013(5)	O(10)–Co(1)–O(10)#1	180.000(1)
Co(1)–O(9)	2.121(4)	O(7)–Co(2)–O(5)	123.6(2)
Co(1)–O(10)	2.157(4)	O(7)–Co(2)–O(9)	139.3(2)
Co(2)–O(7)	1.974(5)	O(5)–Co(2)–O(9)	94.46(19)
Co(2)–O(5)	1.988(5)	O(7)–Co(2)–N(1)#2	95.0(2)
Co(2)–O(9)	2.012(4)	O(5)–Co(2)–N(1)#2	90.1(2)
Co(2)–N(1)#2	2.071(6)	O(9)–Co(2)–N(1)#2	99.3(2)
Co(2)–O(10)#1	2.204(5)	O(7)–Co(2)–O(10)#1	87.1(2)
Co(3)–N(6)	2.102(6)	O(5)–Co(2)–O(10)#1	90.50(19)
Co(3)–O(2)	2.134(5)	O(9)–Co(2)–O(10)#1	77.73(17)
Co(3)–O(3)	2.135(5)	N(1)#2–Co(2)–O(10)#1	177.0(2)
O(6)–Co(1)–O(6)#1	180.00(17)	N(6)#3–Co(3)–N(6)	180.000(3)
O(6)–Co(1)–O(9)#1	88.89(18)	N(6)–Co(3)–O(2)#3	87.7(2)
O(6)–Co(1)–O(9)	91.11(18)	N(6)–Co(3)–O(2)	92.3(2)
O(6)#1–Co(1)–O(9)	88.89(18)	O(2)#3–Co(3)–O(2)	180.0(3)
O(9)#1–Co(1)–O(9)	180.000(1)	N(6)–Co(3)–O(3)#3	89.1(2)
O(6)–Co(1)–O(10)	93.01(19)	O(2)–Co(3)–O(3)#3	89.4(2)
O(9)–Co(1)–O(10)#1	76.48(17)	N(6)–Co(3)–O(3)	90.9(2)
O(9)–Co(1)–O(10)	103.52(17)	O(2)–Co(3)–O(3)	90.6(2)
O(6)–Co(1)–O(10)#1	86.99(19)	O(3)#3–Co(3)–O(3)	180.000(2)
2			
Zn(1)–O(2)	1.937(5)	O(2)–Zn(1)–N(2)	113.6(2)
Zn(1)–O(4)#1	1.985(5)	O(4)#1–Zn(1)–N(2)	106.2(3)
Zn(1)–N(2)	2.002(6)	O(2)–Zn(1)–N(6)	95.3(2)
Zn(1)–N(6)	2.022(6)	O(4)#1–Zn(1)–N(6)	103.6(2)
O(2)–Zn(1)–O(4)#1	115.2(2)	N(2)–Zn(1)–N(6)	122.8(3)
3			
Mn(1)–O(4)	2.098(2)	O(2)–Mn(1)–N(1)#2	86.87(10)
Mn(1)–O(5)#1	2.132(3)	O(4)–Mn(1)–N(7)	96.74(11)
Mn(1)–O(2)	2.239(2)	O(5)#1–Mn(1)–N(7)	93.43(11)
Mn(1)–N(1)#2	2.252(3)	O(2)–Mn(1)–N(7)	88.71(10)
Mn(1)–N(7)	2.283(3)	N(1)#2–Mn(1)–N(7)	175.03(10)
Mn(1)–N(6)	2.360(3)	O(4)–Mn(1)–N(6)	88.34(11)
O(4)–Mn(1)–O(5)#1	106.24(11)	O(5)#1–Mn(1)–N(6)	165.01(10)
O(4)–Mn(1)–O(2)	165.80(10)	O(2)–Mn(1)–N(6)	78.71(10)
O(5)#1–Mn(1)–O(2)	86.42(10)	N(1)#2–Mn(1)–N(6)	88.77(11)
O(4)–Mn(1)–N(1)#2	87.06(11)	N(7)–Mn(1)–N(6)	88.15(11)
O(5)#1–Mn(1)–N(1)#2	88.55(11)		

Note: Symmetry transformations used to generate equivalent atoms for 1: #1: $-x, -y+1, -z+1$; #2: $x-1, y, z$; #3: $-x, -y+2, -z+2$; for 2: #1: $-x+3/2, y-1/2, z-1/2$; for 3: #1: $-x, -y+1, -z+1$; #2: $x-1, y, z$.

Table 3. Hydrogen-bonding parameters for **1–3**.

D–H···A	D–H (Å)	H···A (Å)	D···A (Å)	∠(DHA) (°)
Compound **1**				
O1–H1···O4#1	0.82	1.92	2.732(8)	168.9
O2–H2C···O4	0.85	1.84	2.679(8)	168.5
O2–H2B···N6#2	0.85	2.48	2.952(8)	115.4
O7–H7B···O11#4	0.85	1.74	2.583(8)	172.4
O7–H7C···O8#3	0.82	1.82	2.669(7)	172.5
O12–H12A···O2#5	0.85	2.09	2.883(10)	155.7
O12–H12B···O11#6	0.85	2.11	2.905(11)	156.2
Compound **2**				
O1–H1···O6#1	0.82	2.03	2.790(9)	153.1
O6–H6A···O4#2	0.85	2.19	3.038(11)	172.5
O6–H6B···O5#3	0.85	1.85	2.695(11)	170.3
Compound **3**				
O1–H1···O7#1	0.82	1.90	2.709(3)	167.3
O2–H2B···N12#2	0.85	2.09	2.931(4)	169.2
O2–H2C···O8#3	0.85	1.81	2.646(4)	168.4
O3–H3···O6#1	0.82	1.82	2.615(3)	163.9
O8–H8C···O3#3	0.85	1.99	2.823(4)	165.6
O8–H8D···O6#4	0.85	1.92	2.755(4)	165.3

Note: Symmetry transformations used to generate equivalent atoms for 1: #1: $x+1, y, z$; #2: $-x, -y+2, -z+2$; #3: $-x-1, -y+1, -z+1$; #4: $-x, -y+1, -z+1$; #5: $x+1, y, z-1$; #6: $-x+1, -y+1, -z+1$; for 2: #1: $-x+2, -y, z-1/2$; #2: $-x+3/2, y-1/2, z-1/2$; #3: $-x+3/2, y-1/2, z+1/2$; for 3: #1: $x+1, y, z-1$; #2: $-x+1, -y+1, -z$; #3: $-x+1, -y+1, -z+1$; #4: $x+1, y, z$.

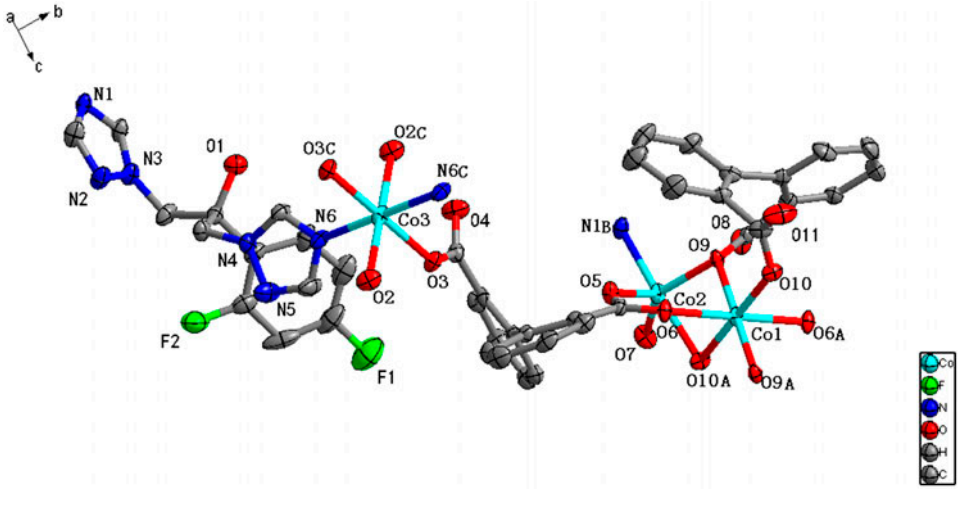

Figure 1. Structure of **1** with 30% probability thermal ellipsoids (hydrogen atoms omitted for clarity). Symmetry codes: A: $-x, 1-y, 1-z$; B: $-1+x, y, z$; and C: $1+x, y, -1+z$.

four O atoms, O10, O10A, O9, and O9A, compose the equatorial plane, while two O atoms, O6 and O6A, are axial. The Co–O bond lengths range from 2.013(5) to 2.157(4) Å. The Co2 atom is five-coordinate with a trigonal bipyramid coordination geometry, defined by four O atoms (O5, O9, O10A, O7) from three different dpa^{2-} anions and one water

molecule, and one N atom N1B from one HFlu ligand. The bond length of Co2–O10A is 2.204(5) Å, and the other Co–O bond lengths range from 1.974(5) to 2.012(4) Å. The bond length of Co2–N1B is 2.071(6) Å. The Co3 atom is six coordinate in a distorted octahedral coordination geometry by four O atoms (O3, O3C, O2, O2C) from two different dpa^{2-} ligands and two different water molecules, with Co3–O bond lengths of 2.134(5) and 2.135 (5) Å, and two N atoms (N6 and N6C) from two distinct HFlu ligands with a Co3–N bond length of 2.102(6) Å. The equatorial plane is composed of the four O atoms O3, O3C, O2, O2C, and the axial positions are occupied by the two N atoms N6 and N6C. All the bond distances above are comparable to the reported values of similar Co-based complexes [24], but the Co–N bond lengths are slightly shorter than the Co–N bond lengths (2.126 (2)–2.204(2) Å) in $\{[Co_2(fcz)_4(H_2O)_4][\beta\text{-}Mo_8O_{26}]\cdot 5H_2O\}$ [fcz = HFlu] [25], which may result from the different coordination modes. In the latter species, there are four N atoms from four HFlu ligands and two water molecules coordinating to each Co(II) atom. Compared to **1**, this may lead to steric repulsion between the ligands, resulting in longer Co–N bond lengths. The three Co(II) atoms (Co1, Co2, Co2A) are connected by the dpa^{2-} ligands to form a trinuclear Co(II) unit (figure 2). The trinuclear Co(II) unit and the Co3 atom are further linked by a dpa^{2-} ligand to form a 1-D serrated structure (figure 3). The HFlu ligand links adjacent 1-D structure into a wave-shaped 2-D-network (figure 4). Within the trinuclear Co(II) unit, the intermetallic distances of Co1–Co2 and Co2–Co2A are 3.20 and 6.40 Å, respectively. The Co–Co intracluster separations are approximately equal to those of reported trinuclear cobalt(II) carboxylate complexes based on the dpa^{2-} ligand, such as $[Co_3(dpa)_2(Hdpa)_2(1\text{-MeIm})_2(H_2O)_2]$ and $\{[Co_3(L)_2(dpa)_2(H_2O)_2]\cdot H_2O\}$ (1-MeIm = 1-methylimidazole; HL = 3,5-di(imidazol-1-yl)benzoic acid) [24, 26]. The Co1–Co3 distance connected by a dpa^{2-} ligand is 9.619 Å, and the Co2–Co3 distance connected by HFlu ligands is 11.322 Å. Both carboxylate groups of the dpa^{2-} ligands are completely deprotonated, adopting. $\mu_2\text{-}\eta^1:\eta^1$ bridging [Co(2)–O(5)–C(27)–O(6)–Co(1)], $\mu_2\text{-}\eta^2:\eta^0$ bridging [Co(2)–O(9)–Co(1); Co(2)–O(10)–Co(1)], and $\mu_1\text{-}\eta^1:\eta^0$ monodentate [Co(3)–O(3)] coordination modes. Although some 2-D-network structures based on the HFlu ligand have been

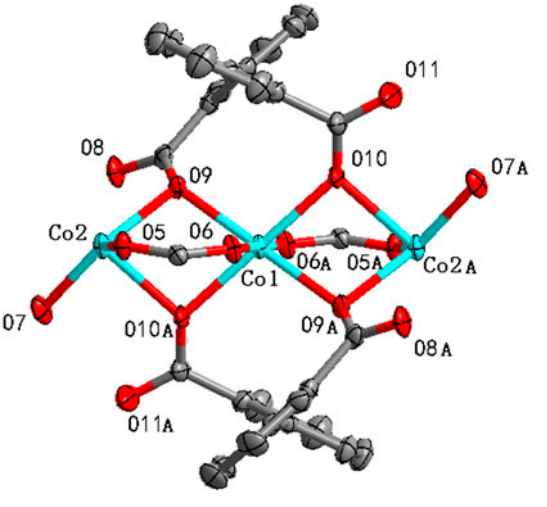

Figure 2. View of the trinuclear Co(II) unit of **1**. Symmetry codes: A: $1+x, y, z$.

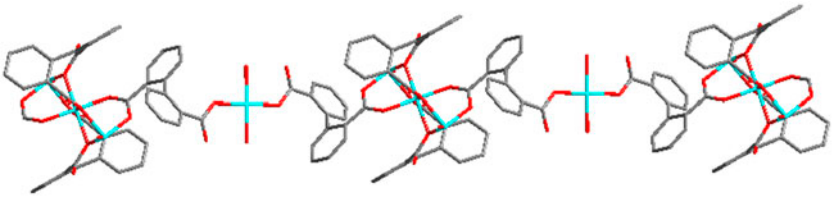

Figure 3. View of the 1-D metal-dpa^{2-} serrated structure.

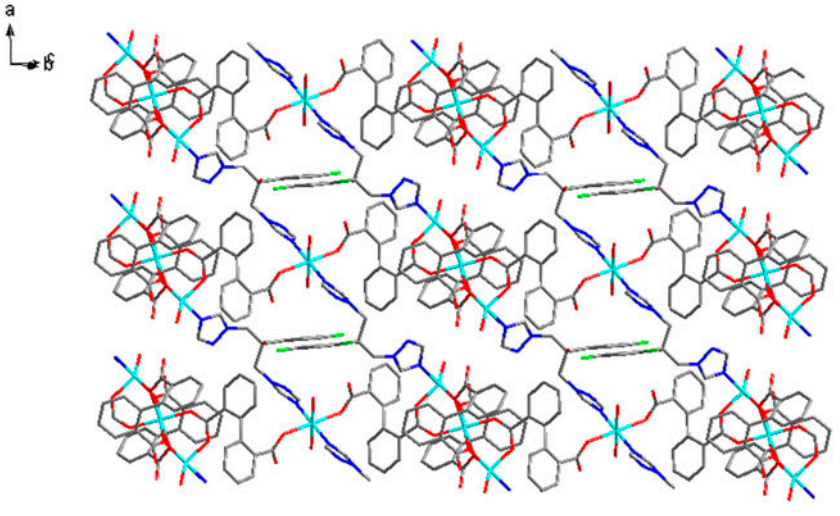

Figure 4. A side view of the 2-D network in **1**.

reported [27]; such a 2-D-network structure with three crystallographic unique Co^{2+} ions and trinuclear Co(II) unit based on HFlu ligand is the first reported. The 2-D-network layers are stacked in an –ABAB– sequence (figure 5).

Water molecules are located between the 2-D layers and further stabilize the structural framework through extensive hydrogen bonding interactions between coordinated water molecules and carboxylate O atoms of dpa^{2-} ligands [O(2)–H(2C)···O(4) 2.679(8); O(7)–H(7C)···O(8)^{i} 2.669(7), (i) $-x-1$, $-y+1$, $-z+1$; O(7)–H(7B)···O(11)^{ii} 2.583(8), (ii) $-x$, $-y+1$, $-z+1$], between coordinated water molecules and the N atoms of the triazolyl group of the HFlu ligand [O(2)–H(2B)···N(6)^{iii} 2.952(8), (iii) $-x$, $-y+2$, $-z+2$], between free water molecules and carboxylate O atoms of the dpa^{2-} ligands [O(12)–H(12B)···O(11)^{iv} 2.905(11), (iv) $-x+1$, $-y+1$, $-z+1$], between free water molecules and coordinated water molecules [O(12)–H(12A)···O(2)^{v} 2.883(10), (v) $x+1$, y, $z-1$], and between carboxylate O atoms of the dpa^{2-} ligands and the hydroxyl O atom of the HFlu ligand [O(1)–H(1)···O(4)^{vi} 2.732(8), (vi) $x+1$, y, z] (figure 6).

Compound **2** is a 3-D framework in the orthorhombic space group Pna2(1) with free water molecules as space fillers. As shown in figure 7, there are one Zn(II) atom, one HFlu ligand, one IPA^{2-} ligand, and one free water molecule in the asymmetric unit. Each Zn(II) center is in a distorted tetrahedral geometry, which is similar to the compound {[Zn(bpp)

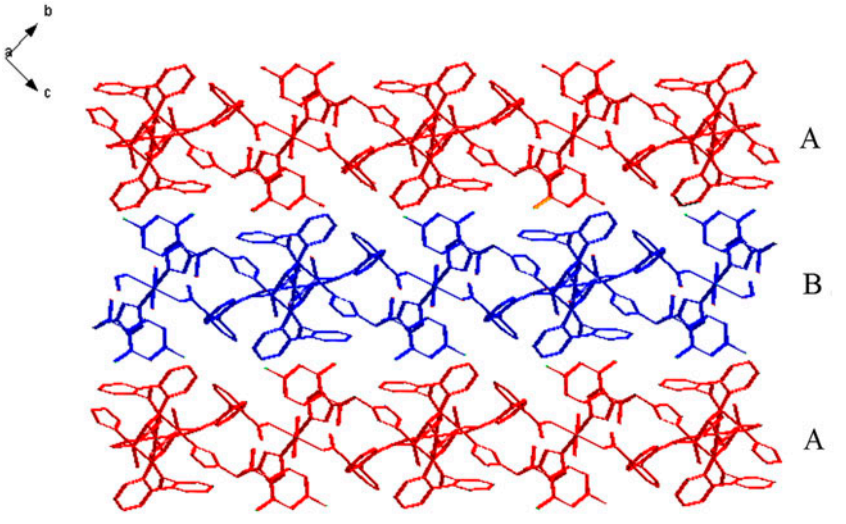

Figure 5. View of the –ABAB– sequence stacking in **1**.

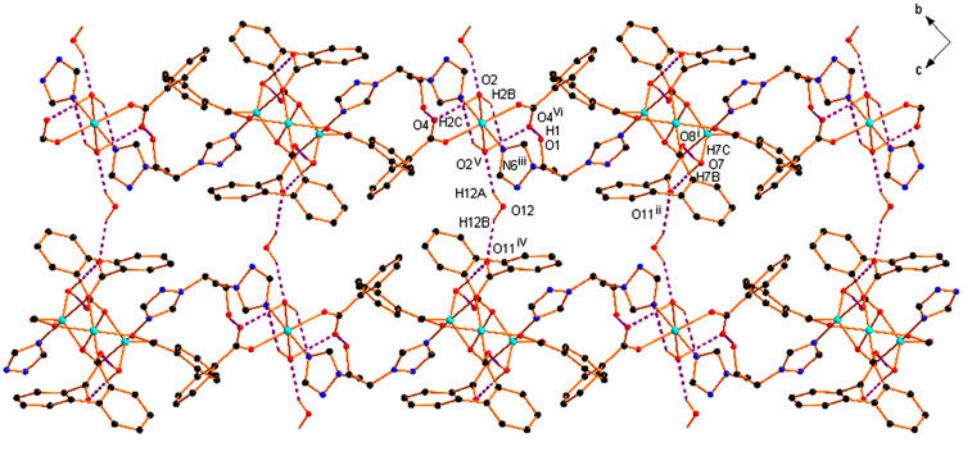

Figure 6. A perspective view of hydrogen bonding interactions in **1** (phenyl groups of HFLu and H atoms not involved in hydrogen bonding are omitted for clarity).

(OH-BDC)](H$_2$O)}$_n$ [OH-H$_2$BDC = 5-hydroxyisophthalic acid; bpp = 1,3-bi(4-pyridyl)propane] [28]. Two N atoms from different HFlu ligands and two monodentate carboxylate O atoms from different IPA^{2-} ligands coordinate to the metal center. The Zn–N distances are 2.002(6) and 2.022(6) Å, and the Zn–O distances are 1.937(5) and 1.985(5) Å. The values of the Zn–N and Zn–O bond distances are comparable to those in {[Zn(bpp)(OH-BDC)](H$_2$O)}$_n$ [28]. The IPA^{2-} ligand is bis-monodentate, bridging two Zn(II) centers to give rise to a 1-D metal-carboxylate wave-shaped chain (figure 8). However, in the reported Zn-based compound containing HFlu, [Zn(HFlu)(TPA)]$_n$ [H$_2$TPA = terephthalic acid] [27], the TPA^{2-} ligand takes bis(bidentate) and bis(monodentate) bridging modes, which is different

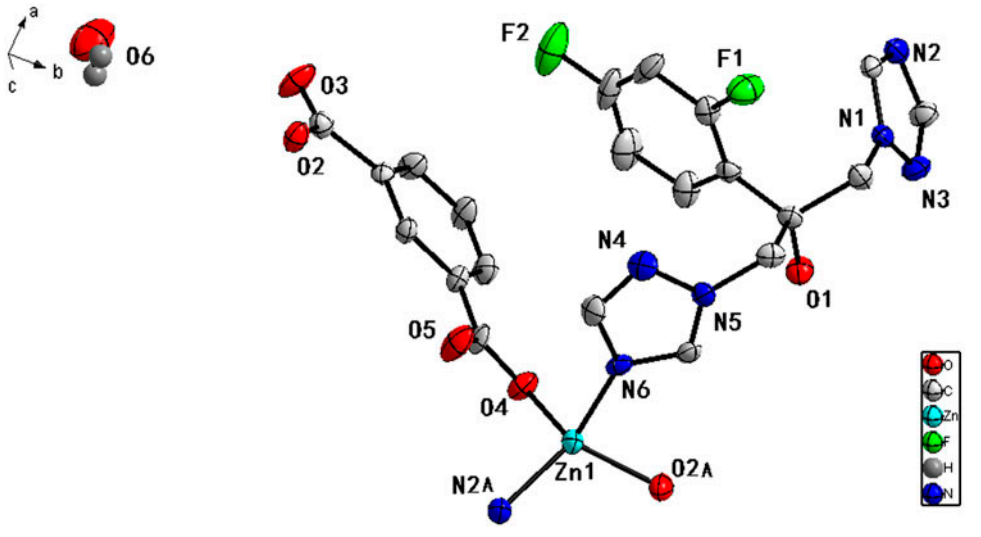

Figure 7. Structure of **2** with 30% probability thermal ellipsoids (hydrogen atoms omitted for clarity except for those of the lattice water molecule). Symmetry codes: A: $1.5 - x$, $0.5 + y$, $0.5 + z$.

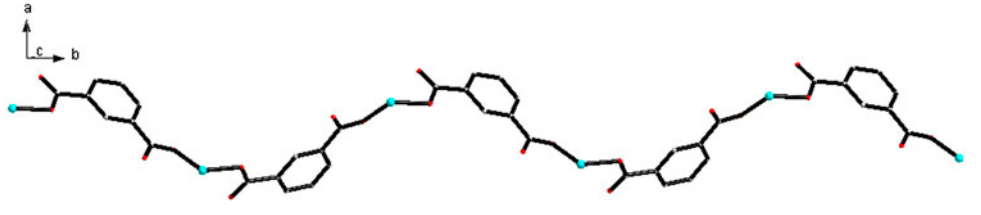

Figure 8. View of the 1-D metal-carboxylate wave-shaped chain in **2**.

from **2**. The coordination and conformation of the HFlu ligand in **2** are comparable with those in $[Zn(HFlu)(TPA)]_n$. In addition, two adjacent 1-D metal-carboxylate wave-shaped chains, stacked along the *a*-axis, in compound **2** are extended in two different directions, forming an angle of 39.26° between the chains when they are viewed orthogonally [figure 9(a)]. The HFlu ligand links these adjacent 1-D chains into a 3-D framework [figure 9(b)]. The Zn–Zn distances bridged by the IPA^{2-} and HFlu ligands are 9.484 and 11.311 Å, respectively. The integration of the HFlu ligand with the IPA^{2-} ligands and Zn(II) atoms does not form quadrangular grids similar to those in $[Zn(HFlu)(TPA)]_n$. Free water molecules are accommodated inside the framework. The hydroxyl group (–OH) of the HFlu ligand does not take part in coordination, but it is involved in a strong hydrogen bonding interaction with a free water molecule (O1–H1···O6^{i} 2.790(9), (i): $x + 1$, y, z), The hydrogen bonding interactions between free water molecules and carboxylate O atoms of the IPA^{2-} ligand [O6-H6A···O4^{ii} 3.038(11), (ii): $-x$, $-y + 2$, $-z + 2$; O6–H6B···O5^{iii} 2.695(11), (iii): $x - 1$, y, z] as well as the hydrogen bonding mentioned above further stabilize the whole structural framework [figures S1 (see online supplemental material at http://dx.doi.org/10.1080/00958972.2014.934229) and 10]. The effective free voids are 6.9% of the structure, with a volume of 157.9 Å^3 in each unit cell [2288.11(6) Å^3] based on a PLATON calculation [29].

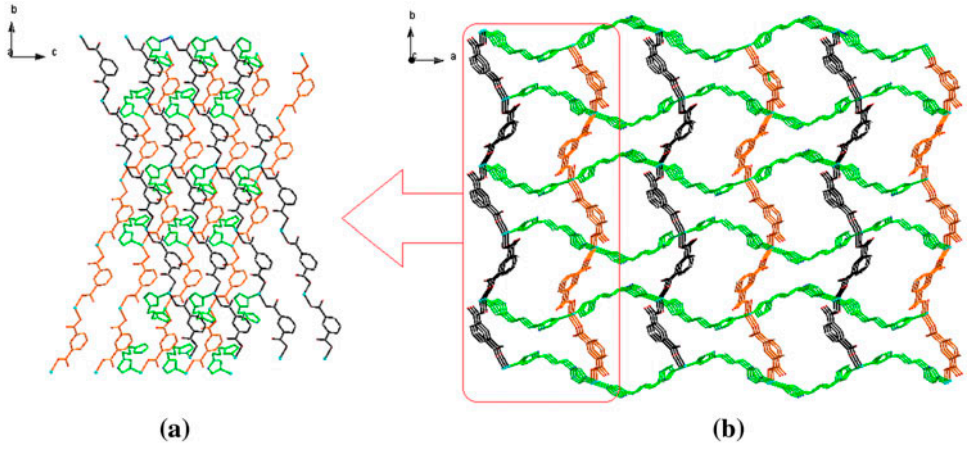

Figure 9. (a) View of the 3-D framework of **2** along the *a*-axis. (b) View of the 3-D framework of **2** along the *c*-axis (the black and orange are the 1-D metal-carboxylate chains; the HFlu ligands are green, the phenyl groups of HFlu omitted for clarity, see http://dx.doi.org/10.1080/00958972.2014.934229 for color version).

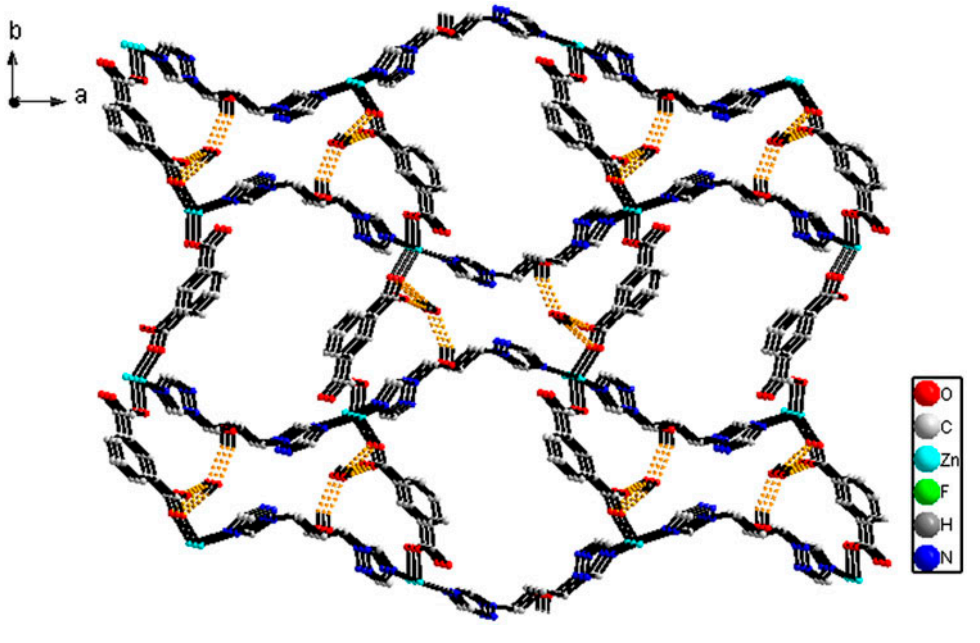

Figure 10. A perspective view of hydrogen bonding interactions in **2** (phenyl groups of HFlu are omitted for clarity).

Single-crystal X-ray diffraction revealed that **3** crystallizes in the triclinic space group $P\bar{1}$ and has a 2-D supramolecular structure through hydrogen bonding interactions between adjacent, 1-D double chain $\{[Mn(HFlu)_2(IPA)(H_2O)\cdot H_2O\}_n$ polymers. The asymmetric unit of **3** contains one Mn(II) atom, two HFlu ligands, one IPA^{2-} ligand, one coordinated water

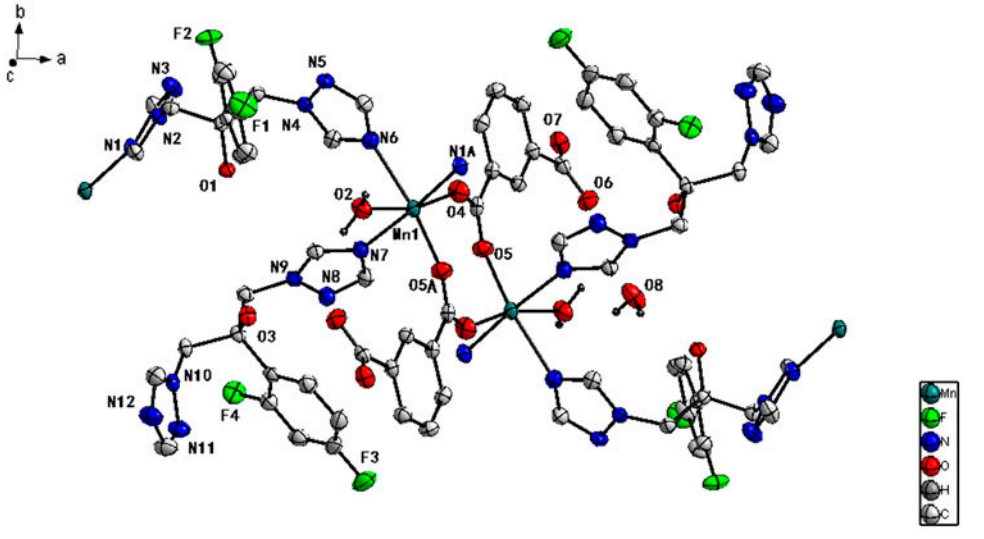

Figure 11. Structure of **3** with 30% probability thermal ellipsoids (hydrogen atoms omitted for clarity except for those of the water molecules). Symmetry codes: (O5) A: $-x$, $1-y$, $1-z$; (N1) A: $-1+x$, y, z.

molecule, and one free water molecule. As shown in figure 11, each Mn(II) atom is six coordinated in a distorted octahedral geometry, by three N atoms from three different HFlu ligands, and three O atom from one coordinated water molecule and carboxylates of two IPA^{2-} ligands. Three N atoms, N1A, N6, and N7, and one O atom O5A make up the equatorial plane, while the two O atoms O2 and O4 are axial. The IPA^{2-} ligands are completely deprotonated; however, only one carboxylate participates in coordination and bridges two Mn atoms in a μ_2-$\eta^1:\eta^1$ coordination mode. The bond lengths of Mn(1)–O(4), M(1)–O(5A), and Mn(1)–O(2) are 2.098(2), 2.132(3), and 2.239(2) Å, respectively. The bond lengths of Mn(1)–N(1A), Mn(1)–N(7), and Mn(1)–N(6) are 2.252(3), 2.383(3), and 2.360(3) Å, respectively. All these bond lengths are slightly longer than the bond lengths for the similar coordination compound bis(μ_2-benzoato-o,o′)-diaqua-bis(tris(pyrazolyl)methane-N,N′,N″)-di-manganese(II) bis(benzoate) (**4**) [30], which may result from steric repulsion between the two HFlu ligands coordinated to each Mn atom in **3**. The two neighboring Mn(II) centers are connected by bridging carboxylate groups of two different IPA^{2-} ligands, which results in the formation of a Mn_2 metallocycle of size 3.179×3.185 Å^2, labeled as [Mn(1)–O(4)–C(27)–O(5)–Mn(1A)–O(4A)–C(27A)–O(5A)] (figure 12). The Mn–Mn distance is 4.484 Å. This distance is 0.21 Å longer than that in **4**, which also has a $[MnO_2C]_2$ metallocycle [30]. Adjacent metallocycles in **3** are connected by two HFlu ligands, generating a 1-D double chain (figure 13). The HFlu ligands adopt two conformers, labeled A (*anti-gauche* conformation) and B (*anti–anti* conformation) [31] in figure 13. While both bond to the Mn_2 metallocycle, only the A-conformer HFlu ligands take part in connecting adjacent metallocycles. The Mn–Mn distance connected by the HFlu ligands is 10.818 Å. Complex **3** forms a 2-D architecture as shown in figure 14, with the help of intermolecular hydrogen bonding [O1–H1···O7#1 2.709(3), #1: $x+1$, y, $z-1$; O2–H2B···N12#2 2.931(4), #2: $-x+1$, $-y+1$, $-z$; O2–H2C···O8#3 2.646(4), #3: $-x+1$, $-y+1$, $-z+1$; O3–H3···O6#1 2.615(3); O8–H8C···O3#3 2.823(4); O8–H8D···O6#4 2.755(4), #4: $x+1$, y, z].

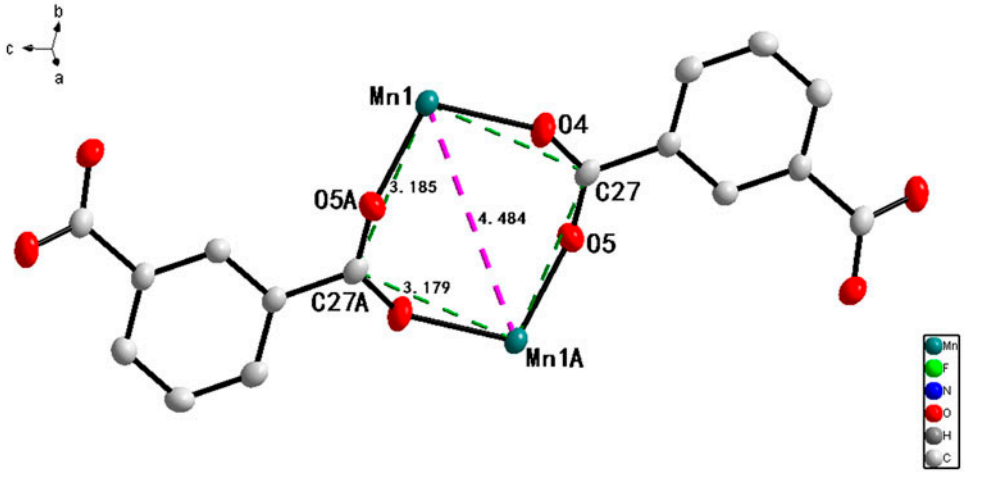

Figure 12. View of the Mn_2 metallocyclic core in **3**.

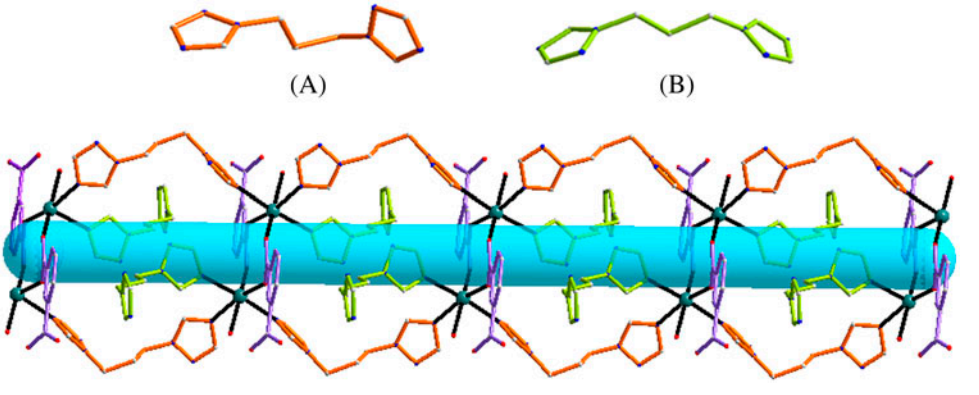

Figure 13. The 1-D chain in **3** (phenyl groups of HFlu omitted for clarity; A: HFlu ligands in the *anti-gauche* conformation; B: HFlu ligands in the *anti–anti* conformation).

3.2. *Infrared spectroscopy*

The IR spectrum of **1** (figure S2) exhibited the characteristic bands of carboxylate groups in the region of 1575–1526 cm^{-1} for the antisymmetric stretch and 1418–1386 cm^{-1} for the symmetric stretch, similar to the Co-based complex $[Co_3(dpa)_2(Hdpa)_2(1\text{-}MeIm)_2(H_2O)_2]$, which showed strong and broad bands in the regions 1598–1532 and 1403–1379 cm^{-1}, for the same vibrations of the coordinated carboxylic groups of the dpa ligands [24]. For **2** (figure S3), the characteristic bands of the carboxylate groups appeared at 1566 and 1356 cm^{-1} for asymmetric and symmetric vibrations, respectively. For **3** (figure S4), the characteristic bands of the carboxylate groups were between 1558–1521 cm^{-1} for the asymmetric vibrations and 1429–1375 cm^{-1} for the symmetric vibrations. The separations (Δ) between $\nu(CO_2)_{asym}$ and $\nu(CO_2)_{sym}$ bands showed that the carboxylate groups are coordinated to the metal atoms. The absence of a characteristic band at around 1700 cm^{-1} in **1–3** indicates the complete deprotonation of carboxylic acid groups of the free ligands [32].

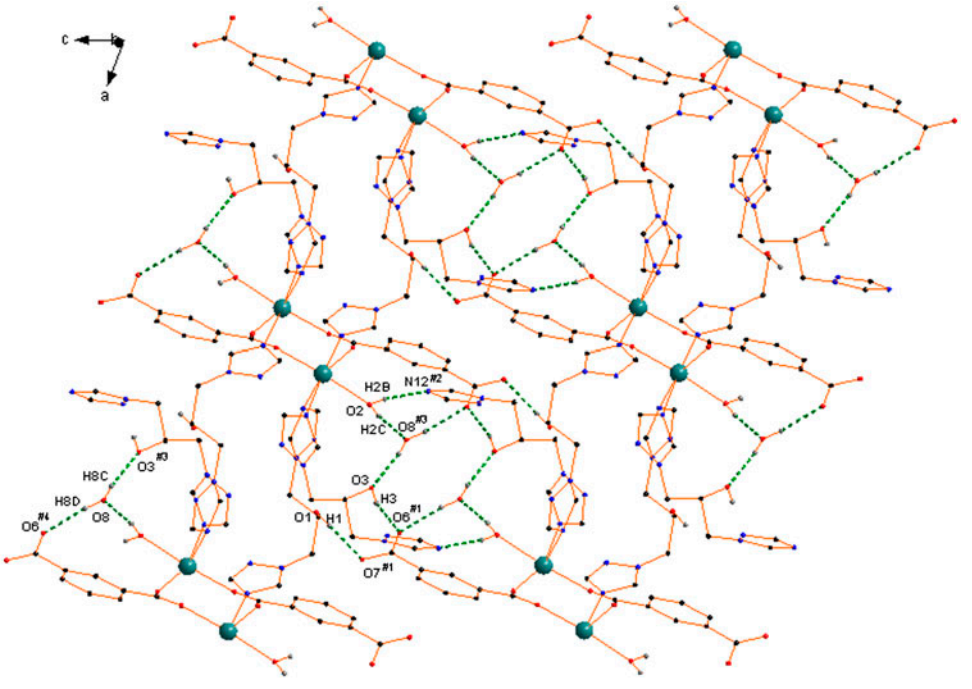

Figure 14. A perspective view of the hydrogen bonding interactions in **3** (phenyl groups of HFlu omitted for clarity).

3.3. *Powder diffraction*

In order to confirm the phase purity of the complexes, the X-ray powder diffraction patterns of **1–3** were measured and are shown in figure 15. It is clearly seen that the peak positions in the experimental PXRD patterns are in good agreement with the corresponding simulated ones except the differences in intensity, which indicates phase purity of each bulk sample. The difference in reflection intensity between the simulated and experimental patterns is due to preferred orientation of the powder samples during data collection.

3.4. *Electronic spectra*

The electronic spectra of **1–3** have bands in the UV/vis-near-IR region (figure 16), arising from various spectroscopic transitions including ligand-centered and metal–ligand charge transfer bands. For **1**, the sharp intense band occurring at 282 nm is attributed to the π–π^* transitions of the ligands, while the bands at 515 and 727 nm are assigned to the LMCT band involving dπCo(II)–π^*(HFlu). For **2**, the sharp intense band centered at 248 nm arises from the π–π^* transition of the ligands. For **3**, the sharp intense band occurring at 260 nm is again attributed to the π–π^* transitions of the ligands, while the bands at 346 and 410 nm are assigned to the LMCT band involving dπMn(II)–π^*(HFlu).

3.5. *Fluorescence properties*

The fluorescence properties of the HFlu and **1–3** have been investigated in solid state at room temperature, and the results are shown in figure 17. Under 253 nm excitation, HFlu

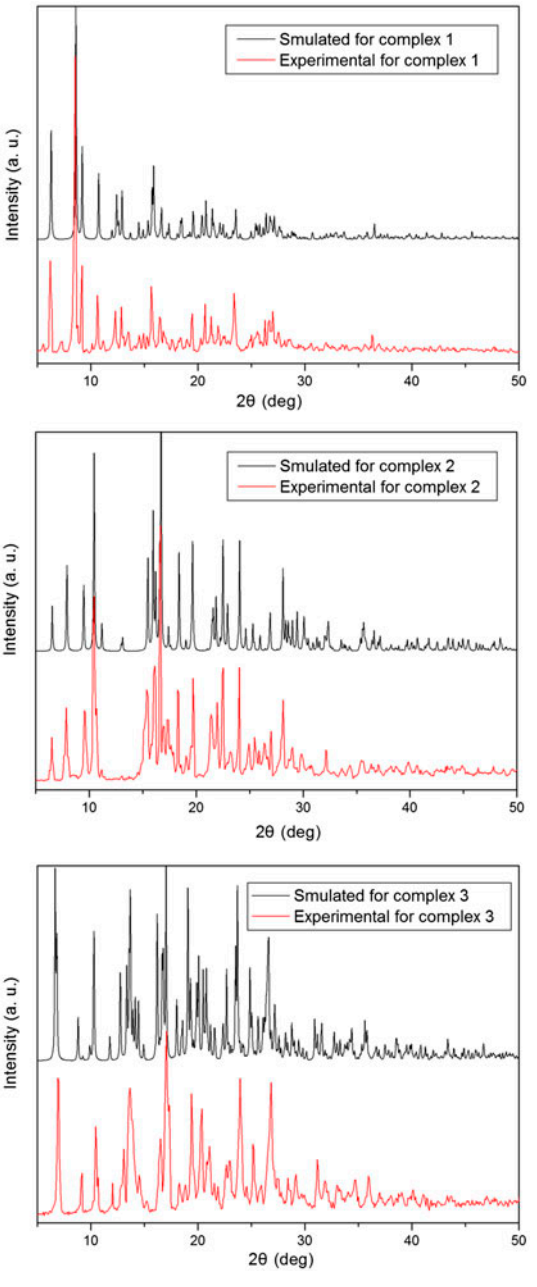

Figure 15. Simulated and experimental PXRD patterns of **1–3**.

emitted strongly at 302 nm, and this is assigned to the $\pi^* \rightarrow \pi$ transition, while **1** gave relatively weak fluorescence at 355 nm under excitation at 226 nm. However, compared with free HFlu, the fluorescence emissions for **1** exhibit a quenching phenomenon, suggesting that HFlu might be used as a luminescent probe to distinguish the dpa^{2-} anion with the

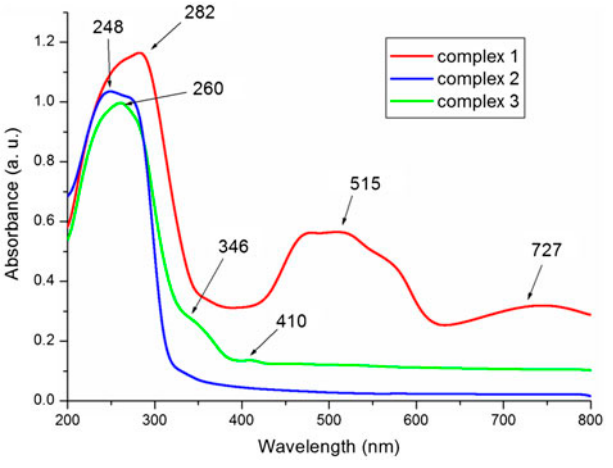

Figure 16. UV–vis spectra of **1–3** in the solid state at room temperature.

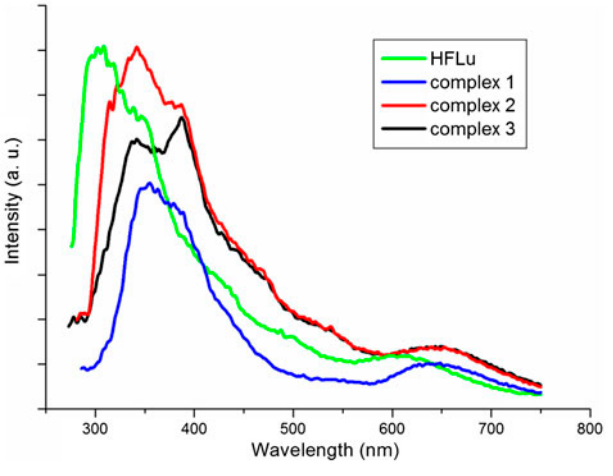

Figure 17. Emission spectra for **1–3** and HFlu in the solid-state at room temperature.

assistance of Co(II) [33]. Complex **2** gives fluorescence at 342 nm upon excitation at 251 nm, and **3** gave fluorescence at 386 nm upon excitation at 234 nm. The emission bands of **1–3** exhibited a red-shift, which probably results from the metal coordination as well as the introduction of dpa^{2-} and IPA^{2-} ligands.

3.6. *Thermal properties*

Complexes **1–3** were subjected to thermogravimetric analysis. As shown in figure 18, **1** displayed the first weight loss of 6.2% in the temperature range of 30–180 °C, corresponding to the loss of one lattice water molecule and two coordinated water molecules (Calcd

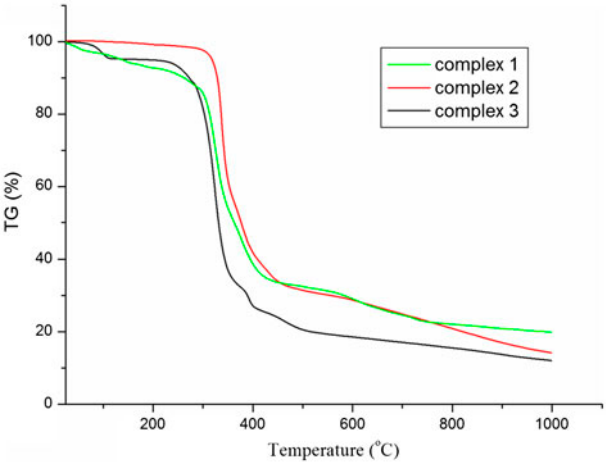

Figure 18. The TGA curves for **1–3**.

5.6%). Continuous heating brought about the pyrolysis of the HFlu and dpa^{2-} ligands. The remaining weight corresponds to the formation of Co_2O_3 (obsd 19.2%, Calcd 17.3%). For **2**, the weight loss of 3.3% before 311 °C can be attributed to the loss of one lattice water molecule (Calcd 3.2%). Further heating led to a sharp weight loss and a rapid framework decomposition. The residue corresponds to the formation of ZnO (obsd 14.4%, Calcd 14.7%). The thermal behavior of **3** consisted mainly three weight loss steps. The first step with 4.5% weight loss from 50 to 120 °C corresponds to the release of lattice water and coordination water molecules (Calcd 4.2%). The second weight loss of 68.9% between 198 and 404 °C corresponds to the pyrolysis processes for the HFlu ligands (Calcd 70.6%). The final weight loss step of 14.9% is consistent with the pyrolysis processes of the IPA^{2-} ligand (Calcd 15.2%), leading to the formation of MnO_2 as the residue (obsd 11.7%, Calcd 10.0%).

4. Conclusion

In summary, we have successfully synthesized three new coordination polymers based on the ligand fluconazole. Complex **1** is a 2-D structure with trinuclear Co(II) units, showing an –ABAB– sequence. Complex **2** is a 3-D framework with free water molecules as space fillers. Complex **3** is a 1-D double chain structure with a dinuclear manganese metallocyclic core. In **1–3**, the HFlu ligand plays an important role in bridging the metal ions through two triazolyl nitrogen donors in head-to-tail mode to form the 2-D, 3-D and 1-D structures, respectively. The auxiliary ligands also play an important part in designing coordination compounds. It is known that multicarboxylate ligands are good candidates for the construction of coordination polymers with specific structures and topologies due to their varied coordination modes [34, 35]. In **1**, the two neighboring carboxylate groups of the dpa^{2-} ligand are known to cooperate in the bridging of the metal ions, so the formation of multi-metal units could be expected. In **2**, the auxiliary IPA^{2-} ligand is coordinated to metal ions

to form a 1-D metal-carboxylate wave-shaped chain, different from other reported isophthalate coordination polymers [36–38]. In these compounds, all the 1-D metal-carboxylate chains are parallel and extend in one direction, while the 1-D metal-carboxylate chains in **2** are and extended in two different directions, at an angle of 39.26° when they are viewed orthogonally. This is a key to further formation of a 3-D structure with the HFlu ligand. In **3**, two Mn(II) atoms are bridged by two IPA^{2-} ligands resulting in a Mn_2 metallocycle, similar to the binuclear secondary building unit of reported compound $[Tm_2(5\text{-}IPA)_4(2,2'\text{-}Hbipy)_2]\cdot 3H_2O$ ($5\text{-}H_2IPA$ = 5-hydroxyisophthalic acid; 2,2′-bipy = 2,2′-bipyridine) [39]. Only one of the two carboxylates of the IPA^{2-} ligand, however, coordinates to Mn(II), which induces the formation of lower dimensional compounds. Complexes **1–3** have also been characterized by IR, UV/vis, and fluorescence spectroscopy and thermal gravimetry. The phase purity of these polymers has been confirmed via the X-ray powder diffraction.

Supplementary material

Figure of the hydrogen bonding interactions in **2** and IR spectra of **1–3**. CCDC-948948, CCDC-951413, and CCDC-951414 contain the supplementary crystallographic data for complexes **1–3**. These data can be obtained free of charge from The Cambridge Crystallographic Data Centre via www.ccdc.cam.ac.uk/data_request/cif.

Funding

This work is supported by the Innovation Project of Guangxi University for Nationalities [grant number gxunchx2013099]; the Natural Science Foundation of Guangxi [grant number 2012GXNSFAA053020]; and the National Natural Science Foundation of China [grant number 20761002], PR China.

References

[1] J.S. Seo, D. Whang, H. Lee, S.I. Jun, J. Oh, Y.J. Jeon, K. Kim. *Nature*, **404**, 982 (2000).
[2] J.J. Perry, G.J. McManus, M.J. Zaworotko. *Chem. Commun.*, **22**, 2534 (2004).
[3] M.D. Bartholomä, A.S. Louie, J.F. Valliant, J. Zubieta. *Chem. Rev.*, **110**, 2903 (2010).
[4] M. Eddaoudi, J. Kim, N. Rosi, D. Vodak, J. Wachter, M. O'Keeffe, O.M. Yaghi. *Science*, **295**, 469 (2002).
[5] J.J. Perry, V.C. Kravtsov, G.J. McManus, M.J. Zaworotko. *J. Am. Chem. Soc.*, **129**, 10076 (2007).
[6] J.P. Li, L.K. Li, H.W. Hou, Y.T. Fan. *Cryst. Growth Des.*, **9**, 4504 (2009).
[7] S.S. Chui, S.M. Lo, J.P.H. Charmant, A.G. Orpen, I.D. Williams. *Science*, **283**, 1148 (1999).
[8] W. Ouellette, J. Zubieta. *Chem. Commun.*, **30**, 4533 (2009).
[9] K. Richardson, K. Cooper, M.S. Marriott, M.H. Tarbit, F. Troke, P.J. Whittle. *Clin. Infect. Dis.*, **12**, S267 (1990).
[10] K. Richardson, K. Cooper, M.S. Marriott, M.H. Tarbit, P.F. Troke, P.J. Whittle, N.Y. Ann. *Ann. N.Y. Acad. Sci.*, **544**, 4 (1988).
[11] L. Zhang, Y. Ling, F. Peng, M. Du. *J. Mol. Struct.*, **829**, 161 (2007).
[12] Y. Ling, L. Zhang, J. Li, A.X. Hu. *Cryst. Growth Des.*, **9**, 2043 (2009).
[13] L. Zhang, Y. Ling, M. Du. *Inorg. Chim. Acta*, **360**, 3182 (2007).
[14] Y. Ling, L. Zhang. *Acta Crystallogr.*, **E63**, m4 (2007).
[15] H.Y. Han, Y.L. Song, H.W. Hou, Y.T. Fan, Y. Zhu. *Dalton Trans.*, 1972 (2006).
[16] Y. Gong, T.F. Liu, W. Tang, F.J. Wu, W.L. Gao, C.W. Hu. *J. Solid State Chem.*, **180**, 1476 (2007).
[17] Y. Gong, W. Tang, W.B. Hou, Z.Y. Zha, C.W. Hu. *Acta Crystallogr.*, **E62**, m1827 (2006).
[18] X.J. Zhao, Q. Wang, M. Du. *Inorg. Chim. Acta*, **360**, 1970 (2007).
[19] Y.Q. Lan, S.L. Li, K.Z. Shao, X.L. Wang, Z.M. Su. *Dalton Trans.*, 3824 (2008).

[20] Y. Gong, J.Z. Liu, C.W. Hu, W.L. Gao. *Inorg. Chem. Commun.*, **10**, 575 (2007).
[21] Y. Gong, C.W. Hu, Z.N. Xia. *J. Mol. Struct.*, **837**, 48 (2007).
[22] G.M. Sheldrick. *SADABS, Program for Empirical Absorption Correction of Area Detector*, University of Göttingen, Germany (1996).
[23] G.M. Sheldrick. *SHELXTL (Version 6.10), Software Reference Manual*, Bruker Instrumentation, Madison, Wisconsin (2000).
[24] I.L. Malaestean, M. Speldrich, S.G. Baca, A. Ellern, H. Schilder, P. Kögerler. *Eur. J. Inorg. Chem.*, **2009**, 1011 (2009).
[25] S.L. Li, Y.Q. Lan, J.F. Ma, J. Yang, X.H. Wang, Z.M. Su. *Inorg. Chem.*, **46**, 8283 (2007).
[26] Z. Su, J. Fan, M. Chen, T. Okamura, W.Y. Sun. *Cryst. Growth Des.*, **11**, 1159 (2011).
[27] L. Zhang, Y. Ling, D.J. Li, J. Li, M. Du. *Inorg. Chim. Acta*, **363**, 1031 (2010).
[28] X. Li, R. Cao, D. Sun, W. Bi, Y. Wang, X. Li, M. Hong. *Cryst. Growth Des.*, **4**, 775 (2004).
[29] A.L. Spek. *Acta Cryst.*, **D65**, 148 (2009).
[30] B. Moubaraki, K.S. Murray, E.R.T. Tiekink. *Z. Kristallogr. New Cryst. Struct.*, **218**, 357 (2003).
[31] Y. Ling, L. Zhang, J. Li, S.S. Fan, M. Du. *CrystEngComm*, **12**, 604 (2010).
[32] L.J. Bellamy. *The Infrared Spectra of Complex Molecules*, Wiley, New York (1958).
[33] L. Zhang, W.W. Chen, Y.Y. Ge, Y. Ling, X.P. Ouyang, J. Li, M. Du. *Inorg. Chim. Acta*, **363**, 866 (2010).
[34] H.S. Choi, M.P. Suh. *Angew. Chem. Int. Ed.*, **48**, 6865 (2009).
[35] C.D. Ene, A.M. Madalan, C. Maxim, B. Jurca, N. Avarvari, M. Andruh. *J. Am. Chem. Soc.*, **131**, 4586 (2009).
[36] P.W. Liu, C.P. Li, Y. Bi, J. Chen. *J. Coord. Chem.*, **66**, 2012 (2013).
[37] J. Xu, X. Sun, C. Ju, L. Yang, C. Bi, M. Sun. *J. Coord. Chem.*, **66**, 2693 (2013).
[38] X. Li, G. Ma, X. Xu. *J. Coord. Chem.*, **66**, 3249 (2013).
[39] F. Zhang, X.T. Huang, Y.Y. Tian, Y.X. Gong, X.Y. Chen, J.J. Lin, D.S. Lu, Y.L. Zhang, R.H. Zeng, S.R. Zheng. *J. Coord. Chem.*, **66**, 2659 (2013).